P. BŁYSKUN*#, J. LATUCH*, T. KULIK*

ISOTHERMAL STABILITY AND SELECTED MECHANICAL PROPERTIES OF $Zr_{48}Cu_{36}Al_8Ag_8$ BULK METALLIC GLASS

The aim of this work was to investigate the influence of isothermal annealing on the amorphous structure stability of the $Zr_{48}Cu_{36}Al_8Ag_8$ alloy. A series of continuous heating examinations was performed on the differential scanning calorimeter in order to determine the temperature limits for isothermal annealing series where the time to crystallization was measured. The obtained results were calculated and a time-temperature-transformation diagram was created and discussed. Static compression test as well as microhardness measurements of the as-quenched samples gave a mechanical properties results supplement. The measured properties (σ_c = 1800 MPa and 614 HV0.05) are comparable to the literature results for this alloy. Fractographic observations with the scanning electron microscope were also performed in order to prove some plasticity observed during the strength tests.

Keywords: bulk metallic glasses, isothermal stability, mechanical properties, TTT curve

1. Introduction

Bulk metallic glasses (BMGs) have already caught a lot of science attention throughout the world. These unique materials are prepared mainly of metals yet exhibit glassy structure. Such combination gives them an extraordinary set of properties. Currently, the most popular BMGs are based on zirconium. They exhibit high mechanical strength as well as very good glass forming ability. Moreover, BMGs have excellent formability due to the superplastic properties at elevated temperature. Even though Zr-based BMGs are still relatively new in human civilization (compared to silica glasses or steels) and they are not yet as well understood as other structural materials, they have already been introduced into the industry as parts of sports goods, springs, electronic casings, etc. [1].

Apart from high purity of alloying elements, high cooling rate of metallic liquid is the first priority during the production of metallic glasses. Simple shapes of relatively low diameter are a natural consequence of the high cooling rate demand. In order to obtain more complicated shapes or larger ingots, one has to use an elevated temperature. Just above the glass transition temperature (T_g) BMGs exhibit supercooled liquid region which is a superplastic substance of a relatively low viscosity. Using this phenomenon is the key to success in BMGs precise components forming [2-5].

Unfortunately, as BMGs are unique, they are also metastable. Any additional energy put into a metastable system may result in a transformation into a more stable state. Processes at elevated temperature are inevitable to use the supercooled liquid region

properties, there is always a risk of its crystallization though. Crystallites are generally avoided in BGMs as they may lead to a mechanical fragility. The temperature where the crystallization begins to occur is defined as T_x. The supercooled liquid region is then limited by T_g and T_x. Annealing time is another factor that adds energy into the system. This means that annealing a BMG in a temperature below T_x for a long time may lead to crystallization as well. Thus, it is important to study this limited stability of the supercooled liquid region carefully in order to achieve repeatable results in BMGs thermo-forming. Some important studies of this issue have already been conducted by Lee et al. [6].

A time-temperature-transformation (TTT) diagram is usually the best choice when processing temperature conditions of an alloy are to be selected. It provides clear and simple information about possible transformations and their time-temperature occurrence. For this reason, authors of this work have made the effort to create a TTT diagram of a Zr-based glass-forming alloy by isothermal annealing processes performed at various temperature levels between T_g and T_x. The $Zr_{48}Cu_{36}Al_8Ag_8$ alloy was selected for this task as it exhibits very good glass forming ability, wide supercooled liquid region and high mechanical properties as well [7-9].

2. Experimental

The master alloy was prepared from high purity elements (6N Zr and 4N in case of other elements) by triple arc melting under argon protective atmosphere with a subsequent removal

*   WARSAW UNIVERSITY OF TECHNOLOGY, FACULTY OF MATERIALS SCIENCE AND ENGINEERING, 141 WOLOSKA STR., 02-507 WARSAW, POLAND

Corresponding author: p.blyskun@inmat.pw.edu.pl

of an oxides layer. It was then vitrified by the copper mould injection casting method. Rod-shaped samples with a diameter of 3 mm were prepared. X-Ray Diffraction method (Rigaku Miniflex2 with Cu K_α radiation) was used to examine the cross-section of these rods to ensure the glassy structure.

At the first stage of thermal studies, the scope of temperature values for supercooled liquid isothermal annealing was to be determined. It is a commonly known fact that the heating rate influences on a phase transformation temperature occurrence, i.e. the higher the heating rate is used, the higher the transformation temperature is observed due to the thermal inertia of an alloy. Thus, a series of continuous heating examinations was performed on the DSC8000 Perkin Elmer calorimeter with the scanning rates of: 0.083, 0.167, 0.333, 0.667, 1.000, 1.333 and 1.667 K/s. Pyris software was used to determine all characteristic temperatures from the obtained DSC curves. It should be underlined here that the T_g was determined in the inflection point of the curve, not in the deflection point.

The glass transition (T_g) and crystallization onset (T_x) temperatures limit the supercooled liquid temperature occurrence. Plotting the T_g versus heating rate allowed to extrapolate this value to 0 K/s heating rate. The Origin environment was used to perform this calculation. Polynomial regression of fourth order was used to fit the T_g values. Obtaining a polynomial equation allowed to calculate a theoretical value of T_{g0} with satisfying accuracy. It was used as a lower limit of an isothermal annealing temperature range. As for the upper limit, it would be the $T_{x\text{-max}}$ measured with a maximum obtainable (by the DSC8000) heating rate (1.667 K/s). At this temperature, during the onset of isothermal annealing mode, crystallization would occur instantly leaving no purpose of examining any higher temperature.

Afterwards, the isothermal annealing was performed at various temperature levels between T_{g0} and $T_{x\text{-max}}$, where the time to the crystallization occurrence was measured in order to describe the supercooled liquid thermal stability. To improve accuracy both T_x and T_p (crystallization peak temperature) were registered as T_x was difficult to be determined when the annealing temperature was relatively low. Each sample was heated from the room temperature to a particular temperature level with a maximum obtainable heating rate (1.667 K/s) and then immediately switched into the isothermal mode. The time was measured from that very moment to the crystallization occurrence. The obtained results were calculated and a time-temperature-transformation (TTT) diagram was created for this alloy.

To supplement the thermal results some mechanical properties of the as-quenched samples were examined as well. Static compression tests were performed on the Zwick testing machine with the strain rate of $5*10^{-4}$ s^{-1} using cylindrical specimens of 3 mm in diameter and 4.5 mm long. The samples were precisely cut and carefully polished with a special holder in order to obtain flat and parallel opposite surfaces. The compression strength of a bulk metallic glass may significantly vary depending on the sample surface quality as well as internal pores and defects distribution. Thus, these tests were repeated three times to improve the statistics. Vickers microhardness was measured on

the Hanemann tester with the load of 0.49 N. This examination took place five times, always on the cross-section near the axis of symmetry of the rod in order to eliminate the influence of the cooling rate differences between internal and lateral areas of the rapidly quenched sample.

After compression tests, some fractographic observations using the scanning electron microscope (Hitachi 3500N) were also performed in order to prove some plasticity observed during the strength tests.

3. Results and discussion

In this work the authors tried to determine the supercooled liquid temperature stability over time in case of the $Zr_{48}Cu_{36}Al_8Ag_8$ alloy. This particular Zr-based composition was selected due to its well known very good glass forming ability and high mechanical properties. This set of properties makes this alloy attractive for both studies and potential structural applications. During simple thermo-mechanical forming processes one can easily alter the shape of the glassy alloy by using the supercooled liquid superplastic properties.

To find the answer to the above considerations, the authors successfully prepared several rod-shaped samples of the rapidly quenched $Zr_{48}Cu_{36}Al_8Ag_8$ alloy made of pure elements by arc melting. XRD pattern of the examined alloy is presented in Fig. 1. None obvious crystalline peaks can be indicated as well as a wide 'halo' can be easily observed proving that the BMG had been successfully manufactured and was fully amorphous.
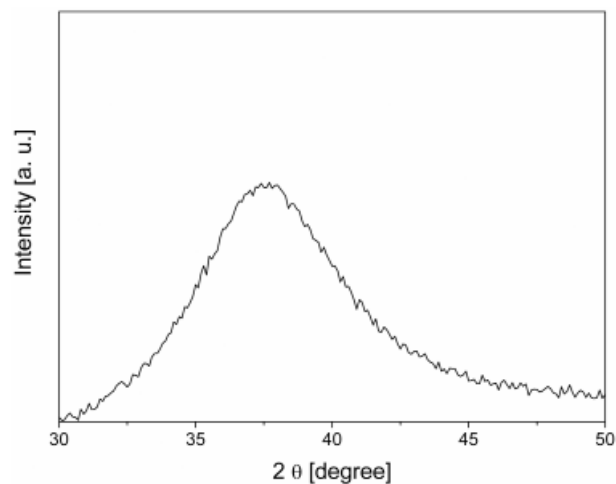

Fig. 1. XRD pattern of the $Zr_{48}Cu_{36}Al_8Ag_8$ alloy in the shape of a rod, 3 mm in diameter

Several series of thermal examinations were carried out using various DSC modes. Firstly, a reasonable temperature range for isothermal annealing experiments was to be determined. The upper and lower temperature limits for the supercooled liquid region are obviously T_x and T_g, respectively. Above T_x the amorphousness begins to vanish and below T_g there is no chance of supercooled liquid occurrence. However, these two

characteristic temperatures strongly depend on the heating rate, thus their values may vary significantly. This means that T_g determined with a relatively high heating rate would give a high temperature value. Surprisingly enough, supercooled liquid state can still occur below it, just lower heating rate have to be applied. The other way around, determination of T_x with a relatively low heating rate would give a low temperature value. However, the supercooled liquid state could survive in a higher temperature for a short period of time if a higher heating rate was used.

For this reason, these limiting temperatures were determined in a series of continuous heating experiments with various heating rates (Fig. 2). It is visible that increasing the heating rate caused all the phenomena to occur at higher temperature. The lower the heating rate was applied, the closer the characteristic temperature value was to the equilibrium one. However, it was obviously not possible to perform such measurements using literally 0 K/s heating rate. Moreover, once crystallization had occurred, these reactions became irreversible. Thus, it was inevitable to predict an absolute value of T_{g0} from T_g vs heating rate plot using an extrapolation function.
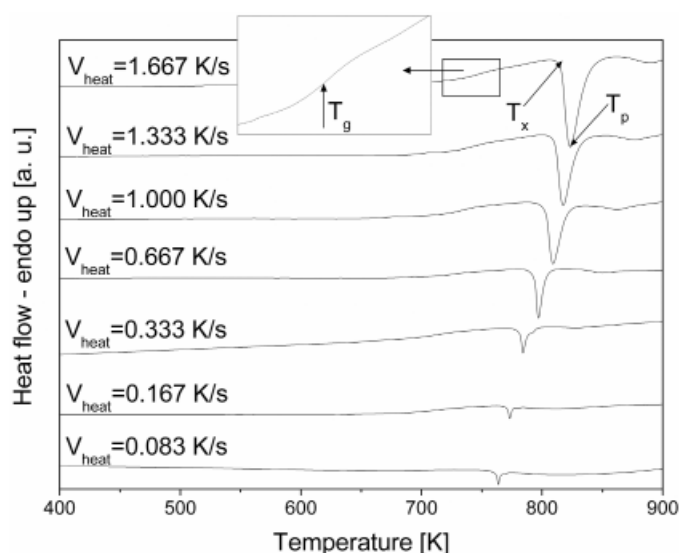

Fig. 2. DSC curves of the $Zr_{48}Cu_{36}Al_8Ag_8$ alloy obtained with a range of heating rates

T_g values determined from curves in Fig. 2 were used to create a T_g vs heating rate plot (Fig. 3). After using a polynomial regression function the absolute value of glass transition temperature could be calculated from the fitting equation: $T_{g0} = 688 \pm 0.5$ K. This value is the lower temperature limit for isothermal annealing as the supercooled liquid should not occur below 688 K in this alloy (regardless of the annealing time).

The assumed method for the isothermal annealing was to heat the sample with a maximum heating rate to a given temperature level and hold it there until it crystallizes. The maximum obtainable heating rate for the DSC8000 is of 1.667 K/s. $T_{x\text{-max}}$ was determined to be of 813 K. Thus, using this equipment, there was no purpose of annealing the sample above 813 K where the crystallization begins immediately after switching the mode to

isothermal annealing. This way, the upper (813 K) and lower (688 K) temperature limits for the next stage of studies were determined.
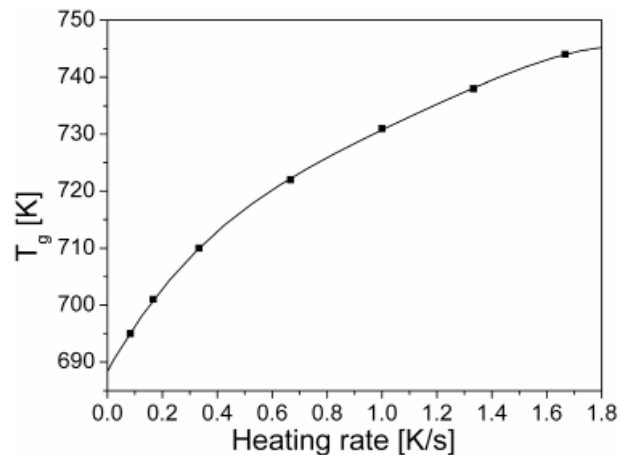

Fig. 3. T_g vs heating rate plot obtained for the $Zr_{48}Cu_{36}Al_8Ag_8$ alloy

The initial isothermal annealing temperature range was determined to be: 688-813 K and scans were planned with a step of 10 K starting from the upper limit. A series of isothermal annealing processes are presented in Fig. 4a,b. These results were split into two groups as the higher temperature annealing processes (Fig. 4b) produced significantly more heat during the crystallization stage while lower ones (Fig. 4a) gave relatively weak signals. Presenting both groups in one plot would seriously hinder correct interpretation of all crystallization peaks. Even with these curves separation, the peak for 723 K in Fig. 4a is still hardly visible. One can notice a disruption in the shape of each curve that appears before crystallization peak. This is a 'noise' background always produced by the DSC when the modes are switched between continuous heating and isothermal annealing (and vice-versa) before the heat flow stabilizes again. This should not be interpreted as a signal from the sample.
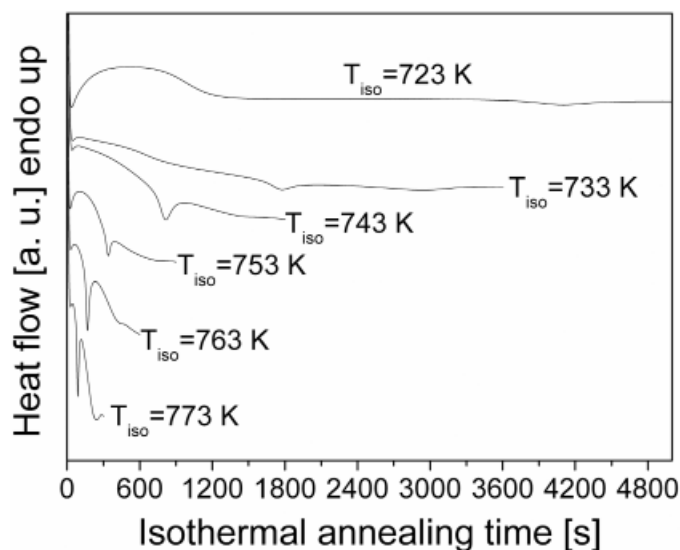

Fig. 4a. Low temperature DSC isothermal annealing curves of the $Zr_{48}Cu_{36}Al_8Ag_8$ alloy
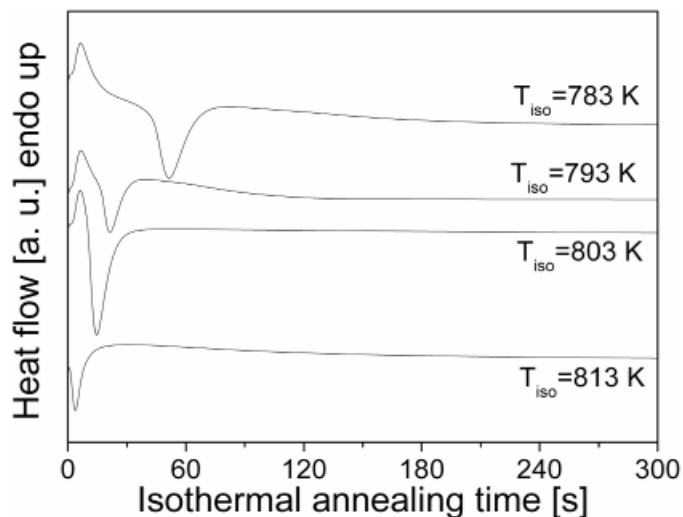
1752

Fig. 4b. High temperature DSC isothermal annealing curves of the $Zr_{48}Cu_{36}Al_8Ag_8$ alloy

Isothermal studies were stopped at 723 K as it had been assumed that one hour should be enough to perform even a complicated thermo-mechanical forming. A crystallization peak temperature (T_p) was easy to determine form the isothermal curves (Fig. 4) and even T_x was calculated with satisfying accuracy. Unfortunately, T_g was not present on the isothermal curves. In order to present at least approximate supercooled liquid stability area, the T_g general trend was calculated from the continuous heating curves. The time consumed to heat the sample to the T_g for each heating rate was used as a rough estimation of the annealing time just to give the image of what it could look like if it was possible to determine T_g from isothermal curves. A time-temperature-transformation diagram of the $Zr_{48}Cu_{36}Al_8Ag_8$ alloy is presented in Fig. 5. T_p was the easiest to determine, thus it is represented by a solid line. T_x determination was slightly more difficult yet still clear, it is then represented by a dashed line. T_g is only a rough estimation, not even based on the isothermal annealing results, so it is just marked with a dotted line.
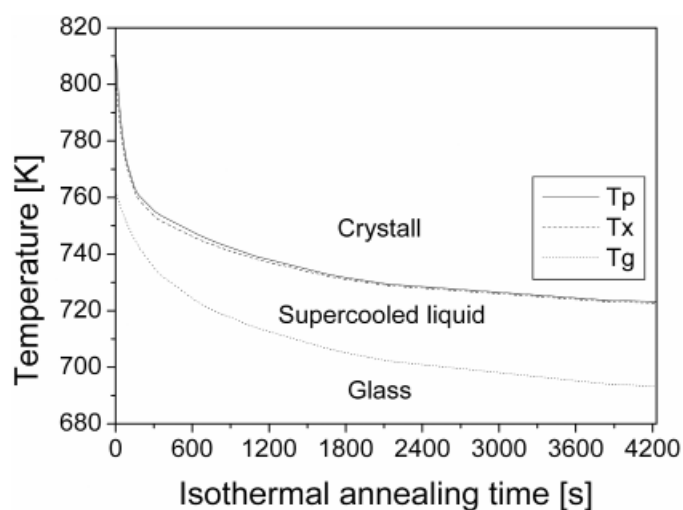

Fig. 5. Supercooled liquid stability presented by TTT curves of the $Zr_{48}Cu_{36}Al_8Ag_8$ alloy obtained by rapid heating of the solid glass and subsequent isothermal annealing

The shape of the approximated T_g curve seems to be similar to the T_x and T_p curves and all of them exhibit the exponential decay trend. The plot in Fig. 5 gives the information about the supercooled liquid stability of the investigated alloy. For example, heating the alloy with a heating rate of 0.667 K/s from the room temperature up to 723 K would cause the glass transition into supercooled liquid after ~11 minutes of continuous heating. At this temperature level the supercooled liquid is stable for up to another ~60 minutes giving a lot of time to process it (Fig. 6).
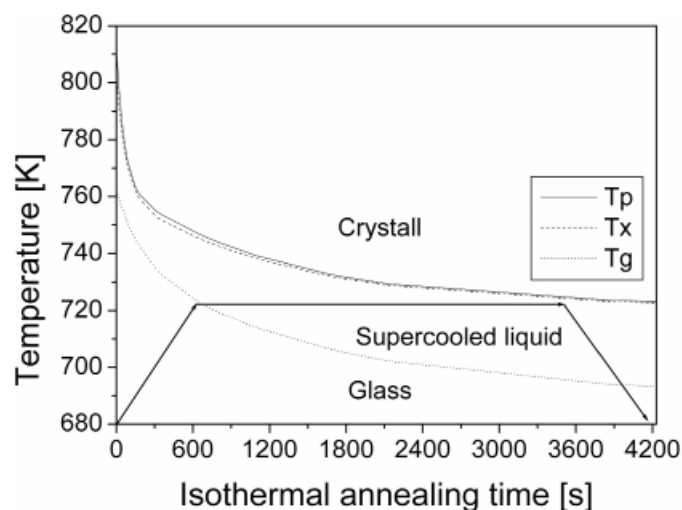

Fig. 6. Processing scheme of the $Zr_{48}Cu_{36}Al_8Ag_8$ alloy based on the TTT curves

Static compression test was performed on three as-quenched samples. An example of obtained strass-strain curve is presented in Fig. 7. One can notice some plastic strain just before the final fracture of the sample. Calculated values of average compression strength, elastic and plastic strains, as well as average microhardness are shown in Table 1 accompanied by the respective values of standard deviation.
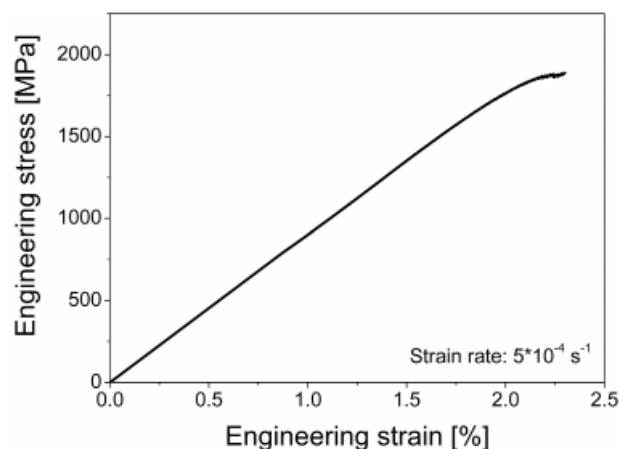

Fig. 7. Engineering stress-strain curve of the $Zr_{48}Cu_{36}Al_8Ag_8$ alloy

Mechanical properties of the investigated alloy determined in this work are comparable to the properties determined by other authors for similar Zr-based alloys [9-15]. High hardness

TABLE 1

Selected mechanical properties of the $Zr_{48}Cu_{36}Al_8Ag_8$ alloy: compression strength (σ_c), elastic strain (ε_{el}), plastic strain (ε_{pl}) and microhardness (HV0.05)

Mechanical property	σ_c [MPa]	ε_{el} [%]	ε_{pl} [%]	HV0.05
	1800	2.0	0.25	614
Standard deviation	±16	±0.1	±0.1	±15

(614 HV0.05), very high compression strength (1800 MPa), extremely large elastic limit (2%) and even some plasticity (0.25% in compression) – this is a very promising set of properties for various structural applications, especially where the elastic energy storage is considered. This alloy combines high mechanical strength and toughness with excellent formability due to large supercooled liquid region and may be an attractive option for some specific applications where price is a secondary criterion.

Fractographic observations were performed on scrap samples after compression tests. Using several magnification levels U-shaped vein-like pattern was observed on the main fracture surface of each sample. There are also some molten droplets visible in the image proving a significant temperature rise resulting from elastic energy release during the fracture [10]. This kind of pattern is typical for a compressed bulk metallic glass and is presented in Fig. 8.
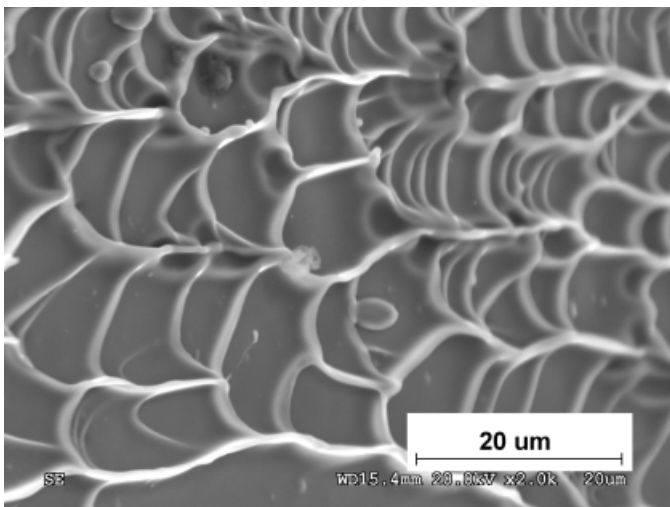

Fig. 8. SEM image showing vein-like pattern of the $Zr_{48}Cu_{36}Al_8Ag_8$ alloy, mag. 2000×

4. Conclusions

The supercooled liquid temperature stability of the $Zr_{48}Cu_{36}Al_8Ag_8$ alloy over time was successfully determined by the isothermal annealing experiment performed at various temperature levels. The obtained results gave an overview of the matter that is relatively easy to interpret and convenient to use: the time-temperature-transformation diagram. The TTT diagram answers the question: for how long can the $Zr_{48}Cu_{36}Al_8Ag_8$ alloy be annealed to avoid crystallization at a given temperature level? For example, at 723 K the supercooled liquid is stable for more than one hour. Using this plot may support temperature level selection to perform thermo-mechanical forming. However, in order to fully understand thermo-forming processes of BMGs, there is a need of further investigations. Strain rate influence on the crystallization rate as well as the temperature level influence on the supercooled liquid net-shaping ability should be well recognized before successful thermo-forming attempts can be made.

The $Zr_{48}Cu_{36}Al_8Ag_8$ alloy exhibits good glass forming ability, excellent mechanical properties and very stable supercooled liquid state, thus it is a promising candidate for both further experiments and industrial applications.

REFERENCES

[1] http://liquidmetal.com
[2] J. Schroers, Adv. Mater. **22** (14), 1566-1597 (2010).
[3] G. Duan, A. Wiest, M.L. Lind, J. Li, W.K. Rhim, W.L. Johnson, Adv. Mater. **19** (23), 4272-4275 (2007).
[4] J.J. Lewandowski, M. Shazly, A. Shamimi Nouri, Scripta Mater. **54** (3), 337-341 (2006).
[5] J.P. Chu, C.L. Chiang, T. Mahalingam, T.G. Nieh, Scripta Mater. **49** (5), 435-440 (2003).
[6] K.S. Lee, Y.S. Lee, J. Mater. Sci. **47**, 2472-2478 (2012).
[7] D.V. Louzguine-Luzgin, G. Xie, S. Li, Q. Zhang, W. Zhang, C. Suryanarayana, A. Inoue, J. Mater. Res. **24** (5), 1886-1895 (2009).
[8] X. Wang, Q.P. Cao, Y.M. Chen, K. Hono, C. Zhong, Q.K. Jiang, X.P. Nie, L.Y. Chen, X.D. Wang, J.Z. Jiang, Acta Mater. **59**, 1037-1047 (2011).
[9] W. Zhang, Q. Zhang, C. Qin, A. Inoue, Mater. Sci. Eng. B **148**, 92-96 (2008).
[10] P. Błyskun, G. Cieślak, M. Kowalczyk, J. Latuch, T. Kulik, Inżynieria Materiałowa **02**, 54-59 (2015).
[11] P. Błyskun, G. Cieślak, M. Kowalczyk, J. Latuch, T. Kulik, Inżynieria Materiałowa **04**, 154-159 (2015).
[12] G. Q. Zhang, Q.K. Jiang, L.Y. Chen, M. Shao, J.F. Liu, J.Z. Jiang, J. Alloys Compd. **424**, 176-178 (2006).
[13] Q. Zhang, W. Zhang, A. Inoue, Scripta Mater. **55**, 711-713 (2006).
[14] A. Inoue, A. Takeuchi, Acta Mater. **59**, 2243-2267 (2011).
[15] Q.K. Jiang, X.D. Wang, X.P. Nie, G.Q. Zhang, H. Mac, H.-J. Fecht, J. Bendnarcik, H. Franz, Y.G. Liu, Q.P. Cao, J.Z. Jiang, Acta Mater. **56**, 1785-1796 (2008).